Pramana – J. Phys. (2016) 87: 20
DOI 10.1007/s12043-016-1222-x

Nonlinear Rayleigh–Taylor instability of the cylindrical fluid flow with mass and heat transfer

ALY R SEADAWY[1,3,*] and K EL-RASHIDY[2,3]

[1]Mathematics Department, Faculty of Science, Taibah University, Al-Ula, Saudi Arabia
[2]Mathematics Department, College of Arts and Science, Taif University, Ranyah, Saudi Arabia
[3]Mathematics Department, Faculty of Science, Beni-Suef University, Beni-Suef, Egypt
*Corresponding author. E-mail: aly742001@yahoo.com

MS received 13 April 2015; revised 9 August 2015; accepted 1 October 2015; published online 7 July 2016

Abstract. The nonlinear Rayleigh–Taylor stability of the cylindrical interface between the vapour and liquid phases of a fluid is studied. The phases enclosed between two cylindrical surfaces coaxial with mass and heat transfer is derived from nonlinear Ginzburg–Landau equation. The F-expansion method is used to get exact solutions for a nonlinear Ginzburg–Landau equation. The region of solutions is displayed graphically.

Keywords. Rayleigh–Taylor instability; fluid flow; mathematical methods; Ginzburg–Landau equation.

PACS Nos 44.25.+f; 44; 02.30.Jr; 04.30.Nk; 24.10.Nz

1. Introduction

The problem of stability of liquids when there is mass and heat transfer across the interface has been investigated by several researchers. The heat and mass transfer phenomenon in multiphase flows has applications in many situations such as boiling heat transfer in chemical engineering and in geophysical problems [1–3]. Hsieh observed that the heat and mass transfer phenomenon enhances the stability of the system if the vapour layer is hotter than the liquid layer. Linear stability analysis of the physical system consisting of a vapour layer underlying a liquid layer of an inviscid fluid was carried out by Hsieh [4]. Hsieh [3] established a general formulation of interfacial flow problem with mass and heat transfer and applied it to the Rayleigh–Taylor and Kelvin–Helmholtz instability problems in plane geometry. The linear stability analysis of a liquid–vapour interface (liquid as viscous and motionless and vapour as inviscid) moving with a horizontal velocity is studied in [5]. Nonlinear Kelvin–Helmholtz instability analysis of liquid vapour interface of an inviscid fluid was performed by Lee [6]. He concluded that when the fluids are inviscid, the linear stability was not affected by heat transfer coefficient.

The heat and mass transfer effects on the Rayleigh–Taylor instability of two viscous fluids and how the mass transfer effect stabilizes the interface are investigated in [7]. Asthana and Agrawal [8] investigated the effect of heat transfer on the Kelvin–Helmholtz instability of miscible fluids using viscous potential flow theory. They observed that the heat and mass transfer has a strong stabilizing effect, when the lower fluid is highly viscous and a weak destabilizing effect, when the viscosity of the fluid is low. Kim *et al* [9] studied the capillary instability including the effect of interfacial heat and mass transfer and noted that the interfacial heat and mass transfer phenomenon resists the growth of disturbance waves [10–13]. The nonlinear Rayleigh–Taylor instability of the interface between two viscous, incompressible and thermally conducting fluids in a fully saturated porous medium, when the phases are enclosed between two horizontal cylindrical surfaces coaxial with the interface is discussed in [14]. The perturbation analysis, in the light of the multiple expansions in both space and time, leads to the well-known Ginzburg–Landau equation. The various stability conditions are discussed both analytically and numerically in [15].

The effect of an electric field on the linear Kelvin–Helmholtz instability was studied by Asthana and Agrawal [16]. The considered fluids were dielectric, and the electric field was applied in the streaming direction. They concluded that the tangential electric field stabilizes the interface in the presence of heat and mass transfer, while the ratio of dielectric constant plays a dual role in the stability analysis. The study of the interaction between magnetic fields and electrically conducting fluids is known as magnetohydrodynamics. The effect of magnetic field on the stability of various types of fluid flows is an important domain of study. The effect of a horizontal magnetic field on the stability of a steady flow was studied by Chandrasekhar [17]. Roberts [18] considered the effect of an unsteady magnetic field on the Rayleigh–Taylor instability. Malik and Singh [19] carried out nonlinear analysis of the Kelvin–Helmholtz instability in the presence of a uniform magnetic field, acting along the surface of separation of two moving superposed fluids [20]. Zakaria [21] studied the nonlinear dynamics of magnetic fluids with a relative motion in the presence of an oblique magnetic field.

This paper is organized as follows: In §2, the formulation of the nonlinear Rayleigh–Taylor stability of the cylindrical interface between the vapour and liquid phases of a fluid, when there is a mass and heat transfer across the interface is shown. The exact solutions for the complex Ginzburg–Landau equation are obtained in §3 [22–26]. The conclusion is given in §4.

2. Formulation of the problem and basic equations

We shall use a cylindrical system of coordinates (r, θ, z) so that in the equilibrium state, z-axis is the axis of symmetry of the system. The central solid core has a radius a. In the equilibrium state, the fluid phase 1, of density ρ^1, occupies the region $a < r < R$, and, the fluid phase 2, of density ρ^2 occupies the region $R < r < b$. The temperature at $r = a$, $r = R$ and $r = b$ are taken as T_1, T_0 and T_2 respectively. The bounding surfaces $r = a$ and $r = b$ are taken as rigid.

The interface, after a disturbance, is given by the equation

$$F(r, z, t) = r - R - \eta = 0, \tag{1}$$

where η is the perturbation in the radius of interface from its equilibrium value R, for which the outward normal vector is written as

$$\mathbf{n} = \frac{\nabla F}{|\nabla F|} = \left\{1 + \left(\frac{\partial \eta}{\partial z}\right)^2\right\}^{-1/2} \left(\mathbf{e}_r - \frac{\partial \eta}{\partial z}\mathbf{e}_z\right). \tag{2}$$

We assume that fluid velocity is irrotational in the region so that velocity potentials are ϕ^1 and ϕ^2 for fluid phases 1 and 2. In each fluid phase

$$\nabla^2 \phi^j = 0, \quad j = 1, 2. \tag{3}$$

The solutions for $\phi^j = 0$, $j = 1, 2$ have to satisfy the boundary conditions. The relevant boundary conditions for our configuration are:

(i) On the rigid boundaries $r = a$ and $r = b$:

The normal field velocities vanish on both the central solid core and the outer bounding surface.

$$\frac{\partial \phi^1}{\partial r} = 0 \quad \text{on} \quad r = a, \tag{4}$$

$$\frac{\partial \phi^2}{\partial r} = 0 \quad \text{on} \quad r = b. \tag{5}$$

(ii) On the interface $r = R + \eta(z, t)$:

(1) The conservation of mass across the interface is:

$$\left[\rho\left(\frac{\partial F}{\partial t} + \nabla\phi \cdot \nabla F\right)\right] = 0$$

or

$$\left[\rho\left(\frac{\partial \phi}{\partial r} - \frac{\partial \eta}{\partial t} - \frac{\partial \eta}{\partial z}\frac{\partial \phi}{\partial z}\right)\right] = 0, \tag{6}$$

where $[h]$ represents the difference in a quantity as we cross the interface, i.e., $[h] = h^2 - h^1$, where superscripts refer to upper and lower fluids, respectively.

(2) The interfacial condition for energy is

$$L\rho^1\left(\frac{\partial F}{\partial t} + \nabla\phi \cdot \nabla F\right) = S(\eta), \tag{7}$$

where L is the latent heat released when the fluid is transformed from phase 1 to phase 2. Physically, the left-hand side of (7) represents the latent heat released during the phase transformation, while $S(\eta)$ on the right-hand side of (7) represents the net heat flux, so that the energy will be conserved.

(3) The conservation of momentum balance, by taking into account the mass transfer across the interface, is

$$\begin{aligned}\rho^{(1)}(\nabla\phi^{(1)} \cdot \nabla F)&\left(\frac{\partial F}{\partial t} + \nabla\phi^{(1)} \cdot \nabla F\right)\\ &= \rho^{(2)}(\nabla\phi^{(2)} \cdot \nabla F)\left(\frac{\partial F}{\partial t} + \nabla\phi^{(2)} \cdot \nabla F\right)\\ &\quad + (p_2 - p_1 + \sigma\nabla \cdot \mathbf{n})|\nabla F|^2,\end{aligned} \tag{8}$$

where p is the pressure and σ is the surface tension coefficient, respectively.

By eliminating the pressure by Bernoulli's equation, we can rewrite the above condition (8) as

$$\left[\rho\left\{\frac{\partial\phi}{\partial t}+\frac{1}{2}\left(\frac{\partial\phi}{\partial r}\right)^2+\frac{1}{2}\left(\frac{\partial\phi}{\partial z}\right)^2-\left\{1+\left(\frac{\partial\eta}{\partial z}\right)^2\right\}^{-1}\right.\right.$$
$$\left.\left.\times\left(\frac{\partial\phi}{\partial z}\frac{\partial\eta}{\partial z}-\frac{\partial\phi}{\partial r}\right)\left(\frac{\partial\eta}{\partial t}+\frac{\partial\phi}{\partial z}\frac{\partial\eta}{\partial z}-\frac{\partial\phi}{\partial r}\right)\right\}\right]$$
$$=-\sigma\frac{\partial^2\phi}{\partial z^2}\left\{1+\left(\frac{\partial\eta}{\partial z}\right)^2\right\}^{-3/2}$$
$$+\sigma(R+\eta)^{-1}\left\{1+\left(\frac{\partial\eta}{\partial z}\right)^2\right\}^{-1/2}. \quad (9)$$

To investigate the nonlinear effects on the stability of the system, we employ the method of multiple scales [14–16]. Introducing ε as a small parameter, we assume the following expansion of the variables:

$$\eta=\sum_{n=1}^{3}\varepsilon^n\eta_n(z_0,z_1,z_2,t_0,t_1,t_2)+O(\varepsilon^4), \quad (10)$$

$$\phi^{(j)}=\sum_{n=1}^{3}\varepsilon^n\phi_n^{(j)}(r;z_0,z_1,z_2,t_0,t_1,t_2)+O(\varepsilon^4),$$
$$j=1,2, \quad (11)$$

where $z_n=\varepsilon^n z$ and $t_n=\varepsilon^n t$, $n=0,1,2$.

The linear wave solutions of (3), subject to boundary conditions, yield

$$\eta_1=A(z_1,z_2,t_1,t_2)\mathrm{e}^{i\theta}+\bar{A}(z_1,z_2,t_1,t_2)\mathrm{e}^{-i\theta}, \quad (12)$$

$$\phi^{(1)}=\frac{1}{k}\left(\frac{\alpha}{\rho^{(1)}}-i\omega\right)A(z_1,z_2,t_1,t_2)E^{(1)}(k,r)\mathrm{e}^{i\theta}$$
$$+\text{c.c.}, \quad (13)$$

$$\phi^{(2)}=\frac{1}{k}\left(\frac{\alpha}{\rho^{(2)}}-i\omega\right)A(z_1,z_2,t_1,t_2)E^{(2)}(k,r)\mathrm{e}^{i\theta}$$
$$+\text{c.c.}, \quad (14)$$

where

$$E^{(1)}(k,r)=\frac{I_0(kr)K_1(ka)+I_1(ka)K_0(kr)}{I_1(kR)K_1(ka)-I_1(ka)K_0(kR)}, \quad (15)$$

$$E^{(2)}(k,r)=\frac{I_0(kr)K_1(kb)+I_1(kb)K_0(kr)}{I_1(kR)K_1(kb)-I_1(kb)K_0(kR)}, \quad (16)$$

$\theta=kz_0-\omega t_0$,

with I_m and K_m, $m=0$, 1 are the modified Bessel functions of the first and second kinds, respectively.

Substituting (12)–(14) into (9), we obtain the following dispersion relation:

$$D(\omega,k)=-a_0\omega^2-ia_1\omega+a_2=0, \quad (17)$$

where

$$a_0=\rho^{(1)}E^{(1)}(k,R)-\rho^{(2)}E^{(2)}(k,R),$$
$$a_1=\alpha\{E^{(1)}(k,R)-E^{(2)}(k,R)\},$$
$$a_2=\frac{\sigma k}{R^2}(R^2k^2-1).$$

From the properties of Bessel functions (is always positive), we notice that the coefficients a_0 and a_1 are greater than zero. Applying the Routh–Hurwitz criteria to (17), the condition for stability is $a_2>0$, from which we obtain $k>1/R$. Thus, the system is stable if $k>k_{\mathrm{c}}$, where

$$k_{\mathrm{c}}=\frac{1}{R}. \quad (18)$$

With the use of the first-order solutions, we obtained the equations for the second-order problem

$$\nabla_0^2\phi_2^{(j)}=-2i\left(\frac{\alpha}{\rho^{(j)}}-i\omega\right)E^{(j)}(k,r)\frac{\partial A}{\partial z_1}, \quad j=1,2, \quad (19)$$

where the linear operator ∇_0^2 is defined as

$$\nabla_0^2=\frac{\partial^2}{\partial r^2}+\frac{1}{r}\frac{\partial}{\partial r}+\frac{\partial^2}{\partial z_0^2}.$$

The non-secularity conditions for the existence of the uniformly valid solution are

$$\frac{\partial A}{\partial t_1}+V_{\mathrm{g}}\frac{\partial A}{\partial z_1}=0, \quad (20)$$

and its complex conjugate relation and V_{g} is the group velocity of the wave

$$V_{\mathrm{g}}=\frac{\mathrm{d}\omega}{\mathrm{d}k}.$$

We examine now the third-order problem:

$$\nabla_0^2\phi_3^{(i)}=-\frac{\partial^2\phi_1^{(i)}}{\partial z_1^2}-2\frac{\partial^2\phi_1^{(i)}}{\partial z_0 z_2}-2\frac{\partial^2\phi_2^{(i)}}{\partial z_0 z_2}, \quad i=1,2. \quad (21)$$

On substituting the values of $\phi_1^{(i)}$ from (15)–(16) and $\phi_2^{(i)}$ into (21), we obtain

$$\phi_3^{(j)}=-\frac{1}{k}\left(\frac{\alpha}{\rho^{(j)}}-i\omega\right)\times\left[\frac{1}{2}\{r^2E^{(j)}(k,r)\right.$$
$$-\frac{r}{k}L^{(j)}(kr)-arM^{(j)}(kr)\}$$
$$-\{RE-aM\}rL^{(j)}(kr)+\frac{1}{k}G^{(j)}(kr)$$
$$\times\left\{\frac{a}{2}E^{(j)}(k,a)-(RE-aM)kaE^{(j)}(k,a)\right\}$$
$$-\left\{\frac{R}{2}(E+Rk)+Rk[aF-(RE-aM)]E\right\}$$

$$\times \frac{E^{(j)}(k,r)}{k}\Bigg] \times \frac{\partial^2 A}{\partial z_1^2} e^{i\theta}$$
$$-\frac{i}{k}\{rL^{(j)}(kr) + aF^{(j)}(kr)$$
$$-(RE - aM)E^{(j)}(k,r)\}$$
$$\times \left[\left\{\frac{\alpha}{\rho^{(j)}} - i\omega\right\} \frac{\partial A}{\partial z_2} + \frac{\partial^2 A}{\partial z_1 t_1}\right] e^{i\theta}$$
$$+\frac{E^{(j)}(k,r)}{k}\frac{\partial A}{\partial t_2} e^{i\theta} + \tilde{\phi}_3^{(j)}, \tag{22}$$

where

$$G^{(j)}(kr) = \frac{1}{\gamma^{(j)}}\{I_0(kr)K_1(kR) + K_0(kr)I_1(kR)\}$$

and, for brevity of notations, we used

$$E = E^{(j)}(k,R), \quad M = M^{(j)}(kR),$$
$$F = F^{(j)}(kR), \quad a = a^{(j)}$$

and

$$\begin{aligned}\tilde{\phi}_3^{(j)} = & -kE^{(j)}(k,R) \times \Bigg[2\left\{E^{(j)}(2k,R) - \frac{1}{kR}\right\} B_2^{(j)} \\ & + \Bigg\{-2\left(E - \frac{1}{kR}\right)\left(\frac{\alpha}{\rho^{(j)}} - i\omega\right)\left(\frac{1}{kR} + \frac{\alpha_2}{k}\right) \\ & + \frac{1}{2}\left(1 + \frac{2}{R^2k^2} - \frac{E}{kR}\right)\left(\frac{3\alpha}{\rho^{(j)}} - i\omega\right) - \frac{\alpha}{\rho^{(j)}} \\ & - i\omega + \frac{\alpha}{\rho^{(j)}k^2}\left(4\alpha_2\left(\frac{1}{R} + \alpha_2\right) - 3\alpha_3\right)\Bigg\} A^2 \\ & - \left\{\left(\frac{\alpha}{\rho^{(j)}} + i\omega\right)\left(E - \frac{1}{kR}\right) + \frac{2\alpha\alpha_2}{\rho^{(j)}k}\right\}\frac{A_2}{k}\Bigg] \bar{A} e^{i\theta} \\ & + H_1 E^{(j)}(2kr) e^{2i\theta} + J_1 E^{(j)}(3kr) e^{3i\theta} \\ & + \text{c.c.},\end{aligned} \tag{23}$$

where the arbitrary functions H_1 and J_1 can be determined from boundary conditions.

With the third-order solution, the condition for third-order perturbation to be nonsecular is

$$i\left(\frac{\partial A}{\partial t_2} + V_{\mathrm{g}}\frac{\partial A}{\partial z_2}\right) + P\frac{\partial^2 A}{\partial z_1^2} = QA^2\bar{A} + RA, \tag{24}$$

where

$$P = \frac{1}{2}\frac{\mathrm{d}V_{\mathrm{g}}}{\mathrm{d}k}, \quad R = -\mu\frac{\partial D}{\partial k}\left(\frac{\partial D}{\partial \omega}\right)^{-1},$$

where μ is defined by $k = k_{\mathrm{c}} + \mu\varepsilon^2$ with k_{c} the critical wave number.

It is now appropriate to introduce the transformations

$$\zeta = \varepsilon^{-1}(z_2 - V_{\mathrm{g}}t_2) = \varepsilon(z_1 - V_{\mathrm{g}}t_1) = \varepsilon(z - V_{\mathrm{g}}t)$$

and

$$\tau = t_2 = \varepsilon t_1 = \varepsilon^2 t.$$

Equation (24) is reduced to

$$i\frac{\partial A}{\partial \tau} + P\frac{\partial^2 A}{\partial \xi^2} = QA^2\bar{A} + RA, \tag{25}$$

which is a complex Ginzburg–Landau equation, i.e.

$$P = P_r + iP_i, \quad Q = Q_r + iQ_i \text{ and } R = R_r + iR_i.$$

The stability of a Ginzburg–Landau equation (25) is discussed by Lange and Newell [17], and Matkowsky and Volpert [18]. They showed that stability conditions are

$$P_rQ_r + P_iQ_i \quad \text{and} \quad Q_i < 0, \tag{26}$$

provided that $R_r = 0$.

We notice that the condition $R_r = 0$ is satisfied when $\omega = 0$ and $P_r = Q_r = 0$. In this case, (25) reduces to the nonlinear diffusion equation (figure 1),

$$i\frac{\partial A}{\partial \tau} + P_i\frac{\partial^2 A}{\partial \xi^2} = Q_iA^2\bar{A} + R_iA, \tag{27}$$

where

$$\begin{aligned}Q_i = & \frac{k}{a_i}\Bigg\{\alpha^2\Bigg[\left(N + \frac{1}{R} + \alpha_2 - 2kE\right) \\ & \times \left\{\frac{E(2k,R)E - 1}{\rho}\right\} + \frac{3}{R\rho}\Bigg] \\ & + \frac{\sigma}{R^4}\Bigg[2RN(k^2R^2 - 1) + 4R\alpha_2 \\ & + 7 - \frac{1}{2}k^2R^2(1 - 3k^2R^2)\Bigg],\end{aligned} \tag{28}$$

with

$$N = -\frac{1}{(8k^2R^2 - 2)}\left\{\frac{R^2\alpha^2}{\sigma}\left[\frac{1 + E^2}{\rho}\right] + \frac{k^2R^2 + 2}{R}\right\}.$$

3. Exact solutions for the complex Ginzburg–Landau equation

The complex Ginzburg–Landau equation:

$$i\frac{\partial A}{\partial \tau} + P\frac{\partial^2 A}{\partial \xi^2} = QA^2\bar{A} + RA, \tag{29}$$

where $A = A(\tau, \xi)$, P, Q and R are constants. Let

$$A(\tau, \xi) = \varphi(\tau, \xi)e^{i(\kappa\tau + \omega\xi)}. \tag{30}$$

We get two equations:

$$\frac{\partial \varphi}{\partial \tau} + 2\omega P\frac{\partial \varphi}{\partial \xi} = 0, \tag{31}$$

$$P\frac{\partial^2 \varphi}{\partial \xi^2} - (\kappa + P\omega^2 + R)\varphi - Q\varphi^3 = 0. \tag{32}$$

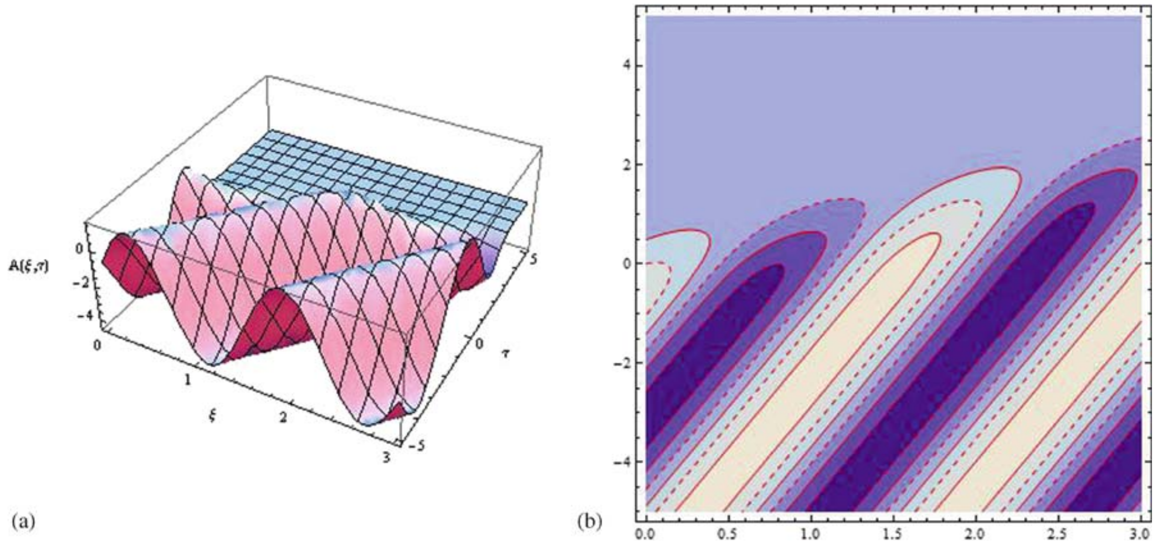

Figure 1. The velocity potential (42) with different shapes are plotted: (**a**) solitary wave solutions, (**b**) contour plot.

Consider the travelling wave solutions $\varphi(\tau, \xi) = \varphi(\zeta)$ and $\zeta = s\tau - \nu\xi$, then eqs (31) and (32) become

$$(s - 2\omega P\nu)\varphi = 0, \tag{33}$$

$$P\nu^2\varphi'' - (\kappa + P\omega^2 + R)\varphi - Q\varphi^3 = 0. \tag{34}$$

The solution of eq. (33) is

$$(s - 2\omega P\nu)\varphi = \zeta + c, \tag{35}$$

where c is the integral constant.

Case 1. Suppose the solutions of eq. (34) are of the form

$$\varphi(\zeta) = a_0 + a_1 F(\zeta), \tag{36}$$

where a_0, a_1 are undetermined constants and $F(\zeta)$ satisfies the ordinary differential equation (ODE)

$$F'^2(\zeta) = \rho^2 F^2(\zeta) + 2\rho\sigma F^3(\zeta) + \sigma F^4(\zeta), \tag{37}$$

where ρ, σ are constants and eq. (37) admits solutions, see [14]:

$$F(\zeta) = -\frac{\rho}{\sigma}\left[\frac{1}{2} - \frac{1}{2}\tanh\left(\frac{1}{2}|\rho|\zeta\right)\right], \text{ if } \rho < 0, \sigma > 0 \tag{38}$$

and

$$F(\zeta) = -\frac{\rho}{\sigma}\left[\frac{1}{2} + \frac{1}{2}\tanh\left(\frac{1}{2}|\rho|\zeta\right)\right], \text{ if } \rho > 0, \sigma < 0. \tag{39}$$

We substitute (36) into eq. (34), using subequation (37) simultaneously. Solving the algebraic equations obtained, yields,

$$a_0 = \pm\frac{\sqrt{-R - \kappa - \omega^2}}{\sqrt{Q}},$$

$$a_1 = \pm\frac{2\sigma(-R - \kappa - \omega^2)^{3/2}}{\rho\sqrt{Q}(R + \kappa + \omega^2)},$$

$$\nu = \pm\frac{\sqrt{2}\sqrt{-R - \kappa - \omega^2}}{\rho\sqrt{P}}. \tag{40}$$

We have solutions to eq. (29) (figures 2, 3 and 4)

$$A(\tau, \xi) = \frac{s\tau - \nu\xi + c}{s - 2\omega P\nu}\mathrm{e}^{i(\kappa\tau + \omega\xi)}, \tag{41}$$

$$A(\tau, \xi) = \left[\pm\frac{\sqrt{-R - \kappa - \omega^2}}{\sqrt{Q}} \pm \frac{(-R - \kappa - \omega^2)^{3/2}}{\sqrt{Q}(R + \kappa + \omega^2)} \times\left(1 - \tanh\left(\frac{1}{2}|\rho|(s\tau - \nu\xi)\right)\right)\right]\mathrm{e}^{i(\kappa\tau + \omega\xi)}, \quad \text{if } \rho < 0, \sigma > 0, \tag{42}$$

$$A(\tau, \xi) = \left[\pm\frac{\sqrt{-R - \kappa - \omega^2}}{\sqrt{Q}} \pm \frac{(-R - \kappa - \omega^2)^{3/2}}{\sqrt{Q}(R + \kappa + \omega^2)} \times\left(1 + \tanh\left(\frac{1}{2}|\rho|(s\tau - \nu\xi)\right)\right)\right]\mathrm{e}^{i(\kappa\tau + \omega\xi)} \quad \text{if } \rho > 0,\ \sigma < 0, \tag{43}$$

where $\rho, \sigma, \nu, \kappa, \omega, R, P$ and Q are arbitrary constants.

Case 2. Suppose the solutions of eq. (34) are of the form

$$\varphi(\zeta) = a_0 + a_1 F(\zeta) + a_2 F^2(\zeta), \tag{44}$$

and $F(\zeta)$ satisfies the ordinary differential equation (ODE)

$$F'^2(\zeta) = \rho F^2(\zeta) + \lambda F^4(\zeta) + \sigma F^6(\zeta). \tag{45}$$

Equation (17) admits solutions, see [14]:

$$F(\zeta) = \left[-\frac{\rho}{\lambda}\left(1 \pm \tanh(\sqrt{\rho}\zeta)\right)\right]^{1/2}, \quad \text{if } \rho > 0, \lambda < 0,\ \lambda^2 = 4\rho\sigma. \tag{46}$$

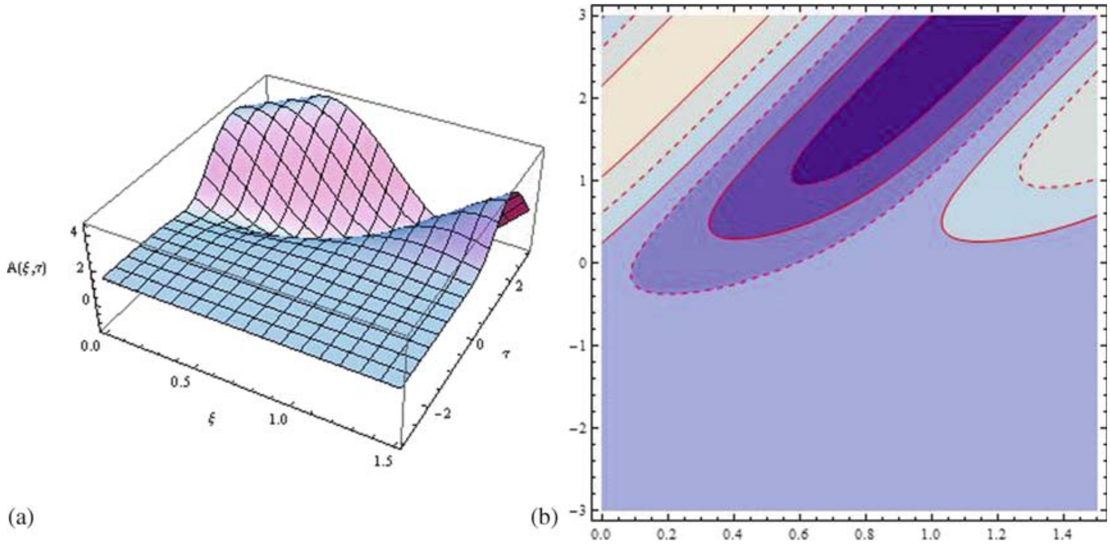

Figure 2. The velocity potential (43) with different shapes are plotted: (**a**) solitary wave solutions, (**b**) contour plot.

We substitute (44) into eqs (34), using subequation (45) simultaneously. Solving the algebraic equations obtained yields (figure 5),

$$a_0 = -\frac{\sqrt{-R-\kappa-\omega^2}}{\sqrt{Q}}, \quad a_1 = 0,$$
$$a_2 = \begin{cases} \dfrac{\lambda(R+\kappa+\omega^2)}{\rho\sqrt{Q}\sqrt{-R-\kappa-\omega^2}}, \\ \dfrac{\lambda\sqrt{-R-\kappa-\omega^2}}{\rho\sqrt{Q}}, \\ \pm\dfrac{\lambda^2(R+\kappa+\omega^2)}{\rho\sqrt{Q}\sqrt{-R-\kappa-\omega^2}}, \end{cases} \tag{47}$$

$$\nu = \pm\frac{\sqrt{-R-\kappa-\omega^2}}{\sqrt{2P\rho}}, \quad \lambda^2 = 4\rho\sigma. \tag{48}$$

We have solutions to eq. (29) (figure 6)

$$A(\tau,\xi) = \left[-\frac{\sqrt{-R-\kappa-\omega^2}}{\sqrt{Q}} - \frac{R+\kappa+\omega^2}{\sqrt{Q}\sqrt{-R-\kappa-\omega^2}} \times \left(1 \pm \tanh(\sqrt{\rho}(s\tau-\nu\xi))\right)\right] \mathrm{e}^{i(\kappa\tau+\omega\xi)}$$
$$\nu = \pm\frac{\sqrt{-R-\kappa-\omega^2}}{\sqrt{2P\rho}}, \quad \rho > 0,\ \lambda < 0,$$
$$\lambda^2 = 4\rho\sigma, \tag{49}$$

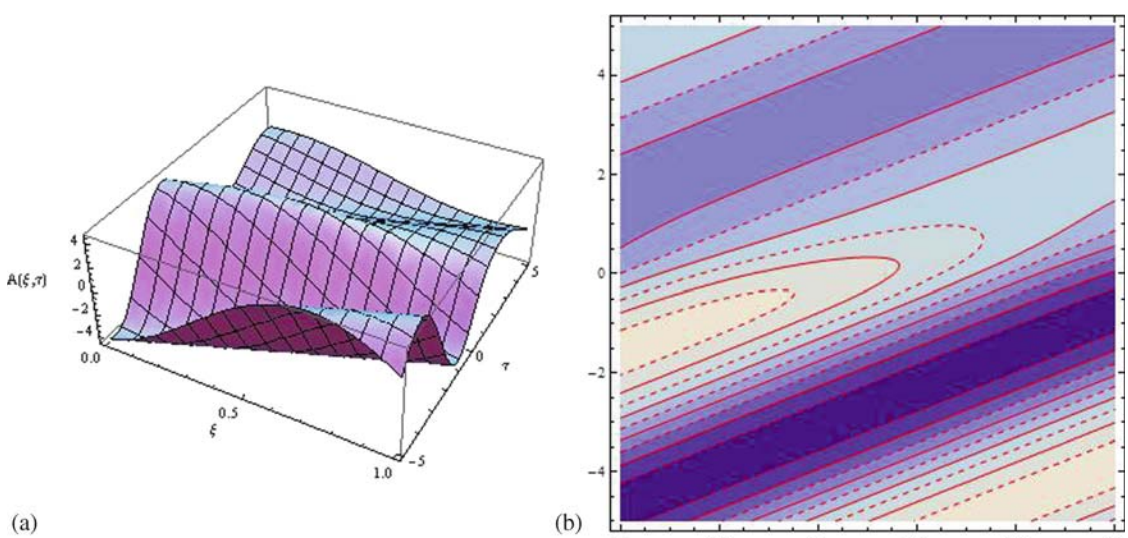

Figure 3. The velocity potential (43) with different shapes are plotted: (**a**) periodic travelling wave solutions, (**b**) contour plot.

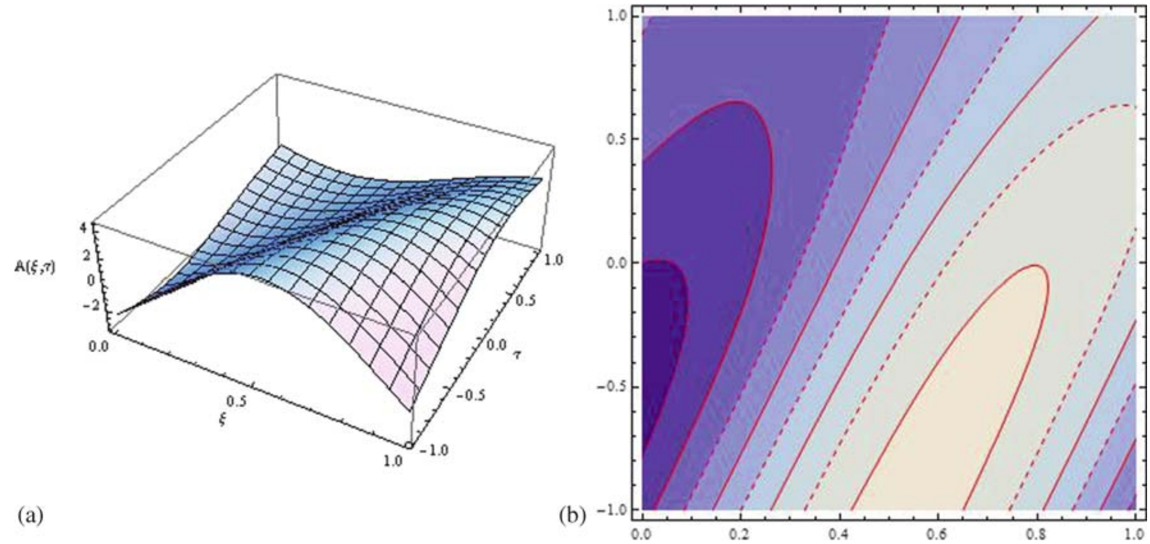

Figure 4. The velocity potential (49) with different shapes are plotted: (**a**) travelling wave solutions, (**b**) contour plot.

$$A(\tau,\xi) = -\frac{\sqrt{-R-\kappa-\omega^2}}{\sqrt{Q}} \times \left[2 \pm \tanh(\sqrt{\rho}(s\tau - \nu\xi)\right] \mathrm{e}^{i(\kappa\tau+\omega\xi)}$$

$$\nu = \pm\frac{\sqrt{-R-\kappa-\omega^2}}{\sqrt{2P\rho}}, \quad \rho > 0, \quad \lambda < 0,$$

$$\lambda^2 = 4\rho\sigma, \tag{50}$$

$$A(\tau,\xi) = \left[-\frac{\sqrt{-R-\kappa-\omega^2}}{\sqrt{Q}} \mp \frac{\lambda(R+\kappa+\omega^2)}{\sqrt{Q}\sqrt{-R-\kappa-\omega^2}}\right] \mathrm{e}^{i(\kappa\tau+\omega\xi)}$$

$$\nu = \pm\frac{\sqrt{-R-\kappa-\omega^2}}{\sqrt{2P\rho}}, \quad \rho > 0, \quad \lambda < 0,$$

$$\lambda^2 = 4\rho\sigma. \tag{51}$$

Case 3. There is a special case, if we take F' as the form:

$$F'^2(\zeta) = \rho^2 F^2(\zeta) + 2\rho\sigma F^4(\zeta) + \sigma^2 F^6(\zeta), \tag{52}$$

where ρ, σ are constants and eq. (52) admits solutions:

$$F(\zeta) = \left[-\frac{\rho}{2\sigma}\left(1 \pm \tanh(\rho^2\zeta)\right)\right]^{1/2},$$

$$\text{if } \rho^2 > 0, \rho\sigma < 0. \tag{53}$$

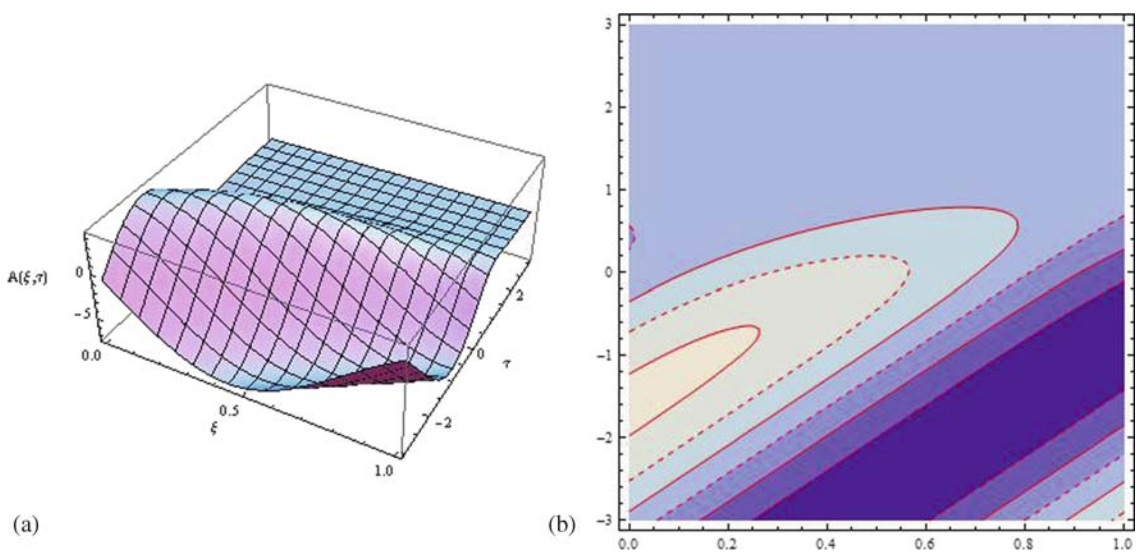

Figure 5. The velocity potential (50) with different shapes are plotted: (**a**) travelling wave solutions, (**b**) contour plot.

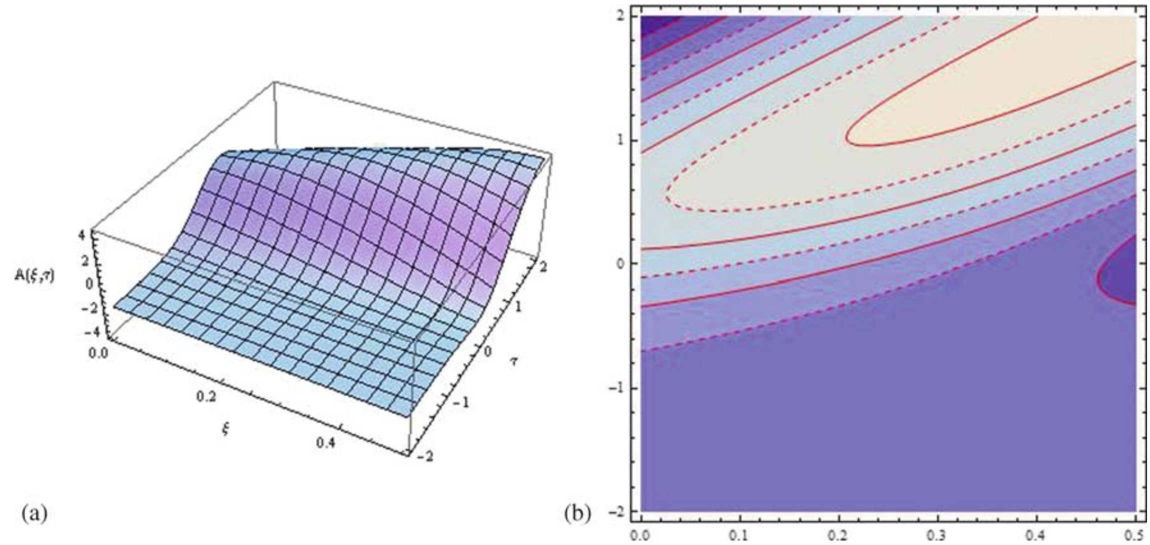

Figure 6. The velocity potential (51) with different shapes are plotted: (**a**) travelling wave solutions, (**b**) contour plot.

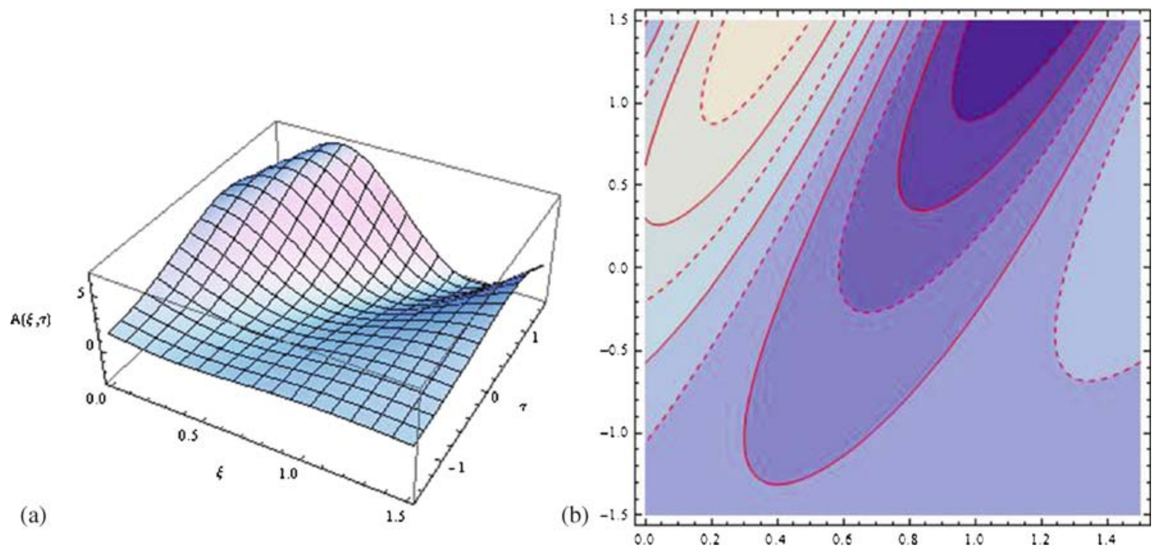

Figure 7. The velocity potential (55) with different shapes are plotted: (**a**) travelling wave solutions, (**b**) contour plot.

We substitute (44) into eq. (34), using subequation (45) simultaneously. Solving the algebraic equations obtained yields (figure 7),

$$a_0 = \pm\frac{\sqrt{-R-\kappa-\omega^2}}{\sqrt{Q}},\quad a_1 = 0,\quad a_2 = \pm\frac{2\nu\sigma\sqrt{2P}}{\sqrt{Q}},$$

$$\rho = \pm\frac{\sqrt{-R-\kappa-\omega^2}}{\nu\sqrt{2P}}. \tag{54}$$

We have solutions to eq. (29)

$$A(\tau,\xi) = \left[\pm\frac{\sqrt{-R-\kappa-\omega^2}}{\sqrt{Q}} \pm \frac{\nu\rho^2\sqrt{2P}}{2\sigma\sqrt{Q}} \times\left(1-\tanh\left(\frac{1}{2}\rho^2(s\tau-\nu\xi)\right)\right)\right]\mathrm{e}^{i(\kappa\tau+\omega\xi)},$$

$$\text{if } \rho<0,\ \sigma>0. \tag{55}$$

4. Conclusion

The nonlinear analysis of Rayleigh–Taylor instability of cylindrical interface between the vapour and the liquid phases of a fluid when there is a mass and heat transfer across the interface was studied. Method of multiple expansions has been used and it is shown that the evolution of the amplitude is governed by the well-known Ginzburg–Landau equation. It is observed that the heat and mass transfer has a stabilizing effect on the stability of the system, while vapour fraction destabilizes the system. By using the F-expansion method, we obtained exact solutions for the nonlinear Ginzburg–Landau equation. The region of solutions was displayed graphically. This is of particular interest for many applications in industrial and environmental processes.

Acknowledgement

This work was supported by the Deanship of Scientific Research, Taibah University, KSA, 2015.

References

[1] D S Lee, *Phys. Scr.* **67**, 420 (2003)
[2] D Y Hsieh, *Phys. Fluids* **21**, 745 (1978)
[3] M K Awasthi, R Asthana and G S Agrawal, *Int. J. Heat Mass Transfer* **78**, 251 (2014)
[4] D Y Heish, *Trans. ASME* **94(D)**, 156 (1972)
[5] K A Khodaparast, M Kawaji and B N Antar, *Phys. Fluids* **7**, 359 (1994)
[6] D S Lee, *J. Phys. A: Math. Gen.* **38**, 2803 (2005)
[7] M K Awasthi and G S Agrawal, *Int. J. Appl. Math. Mech.* **7(12)**, 73 (2011)
[8] R Asthana and G S Agrawal, *Physica A* **382**, 389 (2007)
[9] H J Kim, S J Kwon, J C Padrino and T Funada, *J. Phys. A Math. Theor.* **41(33)**, 335205 (2008)
[10] A H Khater, D K Callebaut, W Malfliet and A R Seadawy, *Phys. Scr.* **64**, 533 (2001)
[11] A H Khater, D K Callebaut and A R Seadawy, *Phys. Scr.* **67**, 340 (2003)
[12] A H Khater, D K Callebaut, M A Helal and A R Seadawy, *Eur. Phys. J. D* **39**, 237 (2006)
[13] A H Khater, D K Callebaut, M A Helal and A R Seadawy, *Phys. Scr.* **74**, 384 (2006)
[14] M K Awasthi, *Int. Commun. Heat Mass Transfer* **56**, 79 (2014)
[15] A H Khater, D K Callebaut and A R Seadawy, *Phys. Scr.* **62**, 353 (2000)
[16] R Asthana and G S Agrawal, *Int. J. Eng. Sci.* **48**, 1925 (2010)
[17] S Chandrasekhar, *Hydrodynamic and hydromagnetic stability* (Dover Publications, New York, 1981)
[18] P H Roberts, *Astrophys. J.* **137**, 679 (1963)
[19] S K Malik and M Singh, *Astrophys. Space Sci.* **109**, 231 (1985)
[20] A R Seadawy, *Physica A* **439**, 124 (2015)
[21] K Zakaria, *Physica A* **327**, 221 (2002)
[22] A R Seadawy, *Comp. Math. Appl.* **62**, 3741 (2011)
[23] A R Seadawy, *Appl. Math. Lett.* **25**, 687 (2012)
[24] A R Seadawy and K El-Rashidy, *Math. Comp. Model.* **57**, 1371 (2013)
[25] A R Seadawy, *Comp. Math. Appl.* **62**, 3741 (2011)
[26] A R Seadawy, *Comp. Math. Appl.* **70**, 345 (2015)